Tautomeric Rearrangements in Mono- and Dichalcogenide Analogs of Formic Acid, HC(X)YH (X, Y = O, S, Se, Te): A Theoretical Study

Eluvathingal D. Jemmis,*,† Kalathingal T. Giju,† and Jerzy Leszczynski*,‡

School of Chemistry, University of Hyderabad, Hyderabad 500 046, India, and Department of Chemistry, Jackson State University, Jackson, Mississippi 39217

Received: March 5, 1997; In Final Form: July 16, 1997[⊗]

Theoretical calculations are reported at the Hartree−Fock (HF), MP2, and Becke3LYP (B3LYP) levels on a complete series of 16 chalcogenic derivatives of formic acid HC(X)YH (X, Y = O, S, Se, Te) using all-electron basis sets. The periodic variations observed on substituting the chalcogens are discussed. The transition structures for the tautomeric rearrangement of these formic acid derivatives are also characterized. The variations in relative energies corrected for zero-point vibrations show that the barrier for tautomerism is reduced as the electronegativity of chalcogens is decreased. The trends of natural charges on atoms of chalcogenides are described. At the correlated level of calculations both MP2 and B3LYP methods give comparable results. The solvent effects on tautomeric equilibrium are assessed by performing self-consistent reaction field (SCRF) calculations at the HF level. A comparative study is provided for two solvation models: the electrostatic solvation model based on Onsager's reaction field theory and the self-consistent isodensity polarized continuum model (SCI-PCM). The latter is shown to be a better model for solvation. The solvents with dielectric constants 2.0, 7.6, and 35.9 are shown to be less effective on the thermodynamic stabilities of these reactions. The dipole moments show significant variations between solvents of lower dielectric medium, while the variations are insignificant between solvents of higher dielectric media. A comparison of thermodynamic preferences for keto and enol forms in monochalcogeno acetc acids with the solvent model SCI-PCM at the HF and B3LYP levels is also provided. Chemical shifts calculated using the GIAO method (at the B3LYP/6-311+G(2D,P)//B3LYP/6-31G(D) level) correlate well with the experimental results. However we conclude from these results that *the thion form of $CH_3C(S)OH$ is less predominant*.

Introduction

The chalcogenide derivatives of carboxylic acids and their applications are an active area of current research.[1−3,4] These derivatives have been helpful in understanding the catalytic activities in biological systems in addition to their general synthetic applications.[2,5] The structures of carboxylic acids and thiocarboxylic acids have been subjected to detailed investigation both experimentally and theoretically.[6−11] On the other hand investigations on carboxylic acids with heavier chalcogens in the carboxylic acid moiety are only developing. The properties of dithiocompounds, −S−C(=S)−, that make them ideal Raman resonance probes[12] are now well-known. Similar studies on diseleno and ditelluro compounds have not reached a comparable level of sophistication. The −C(=X)Y−, (X, Y = O, S, Se, Te) fragments have been found useful as chelate ligands in various organometallic compounds.[3] The nature of chelation in these compounds depends on the strength of the electronic interaction enforced by interacting chalcogen with the coordinating metallic center. It is known that the strength of the C−X bonds decreases in the order O > S > Se > Te. This order of strength followed the C−X and C=X bond lengths and the orbital electronegativities of the carbon and the chalcogens.[1,13] Since steric bulk of the heavier chalcogens Se and Te is large, it was considered that molecules having C−Se and C−Te single and double bonds are very unstable.[14] Despite their proximity to sulfur in various properties, it is not possible to anticipate the chemistry of the heavier analogs due to their greater steric bulk and more polarizability relative to sulfur, especially when they coexist in the same molecule. Simple derivatives of HC(X)YH are primary targets of such studies.

Earlier theoretical and experimental studies on thioformic acids had shown that thiol formic acid (**2**) is more stable than thiono formic acid (**3**).[9,10] On the other hand thiol acetic acid was proved to be less stable than thiono acetic acid polar solution[15] even though theoretical studies at the HF/4-31G level had shown otherwise.[16] But the relative stabilities of monoseleno and monotelluro formic acids are not known. Recently Kato and co-workers reported extensive experimental studies on monochalcogeno carboxylic acids in which S, Se, and Te were substituted for one of the two oxygen atoms of the carboxylic acid.[15] They had concluded that the enol form RC(E)OH (R = alkyl or aryl; E = S, Se, Te) is predominantly present in polar solvents at lower temperatures, while the keto form RC(O)EH is preferred in nonpolar solvents. No theoretical study on these chalcogenide derivatives is available in the literature. In this paper we will consider the theoretical treatment of formic acid and its chalcogenic derivatives at various levels of theory. We study a number of mono- and dichalcogenic formic acid derivatives by replacing one or two oxygens of the carboxylic acid moiety with S, Se, and Te. Such an investigation would give a reasonable understanding of the periodic variations in these systems, which are helpful to the experimentalists. In view of the potential importance in the application of 1,3-H shift in reaction mechanisms, we also analyze the unimolecular tautomerization of these molecules. Several levels of theory are employed to determine the structure of transition states and the barrier heights for the 1,3-H shifts. These include HF, MP2, and density functional methods. We have also tried to investigate the general effect of the solvent on the tautomeric rearrangement among different formic acid derivatives by performing SCRF calculations.

† University of Hyderabad.
‡ Jackson State University.
[⊗] Abstract published in *Advance ACS Abstracts,* September 1, 1997.

S1089-5639(97)00838-4 CCC: $14.00

Theoretical Methods

All calculations were performed using the Gaussian 92/DFT[16] and Gaussian 94[18] suite of programs. The ab initio level of calculations were performed at HF and MP2 (frozen core)[19] levels of theory. The hybrid density functional calculations were performed using the B3LYP functional.[20−23] Geometries for all structures were fully optimized with C_s symmetry constraints at the HF, MP2, and B3LYP levels. The basis used are Pople's 6-311G(2D) for H, C, O, and S,[24] while the Huzinaga's basis sets[25] were modified to (433111/43111/411) for Se and (4333111/433111/4311) for Te. The exponents of d-functions added for Te are 0.096 and 0.305, respectively, while those for Se are 0.144 and 0.489, respectively. A general basis set input with 6D option was used for Se and Te. The analytic harmonic vibrational frequency calculations were done to characterize the nature of stationary points on the potential energy surface (PES) and to estimate the zero-point vibrational energy (ZPE). The ZPE values were scaled by 0.89 at the HF level, by 0.945 at the MP2 level, and 0.98 at the B3LYP level to account for the overestimation of vibrational frequencies at these levels.[26] The scaled ZPE corrections are included in the relative energy (RE) values.

The transition structures (**TS1**−**TS10**) for tautomeric conversions were also located at all three levels considered here. These were characterized with only one imaginary vibrational frequency in each case. The optimized geometries for **TS1**, **TS5**, **TS8**, and **TS10** have C_{2v} symmetry, while other transition structures have C_s symmetry.

The effect of solvent on the structure and the relative stabilities at the tautomeric equilibrium was studied using the self-consistent reaction field (SCRF) method. In the SCRF calculation, we have considered two models. One is the electrostatic solvation model based on Onsager's reaction field theory,[27−29] and the second is the self-consistent isodensity polarized continuum model (SCI-PCM)[30] developed from a reaction field based on the polarized continuum model proposed by Tomasi and co-workers.[31] In the former model, the solute is placed in a uniform electric field of solvent with a dielectric constant ϵ. The solute is assumed to occupy a spherical cavity of radius a_0 in the medium. A dipole in the molecule will induce a dipole on the medium, and the electric field applied to the solute by the solvent dipole in turn interacts with the molecular dipole to lead to net stabilization. This model has a major drawback that the molecule is in a sphere which is usually far away from the realistic picture. The second model (SCI-PCM) has derived some advantage over the drawback of Onsager's model. Here the cavity is defined as an isosurface of the molecule, and the coupling of the isosurface and the electron density are taken fully into account. We have considered various solvents with dielectric constants[30,32] 2.0 (cyclohexane), 7.6 (tetrahydrofuran abbreviated as THF), and 35.9 (acetonitrile abbreviated as MeCN) to understand the effect of dielectric medium on the intramolecular, tautomeric equilibrium. The radius of the spherical cavity for the Onsager's model was calculated by performing single-point calculations at the optimized geometry of the HF level (gas phase) by specifying the keyword VOLUME as in the Gaussian packages. With these cavity radii, the SCRF calculations were performed on the formic acids and their transition structures. The analytic vibrational frequencies were calculated to ascertain the nature of stationary point. The dipole moment values are reported for all minima and transition structures both without and with solvent medium.

SCHEME 1

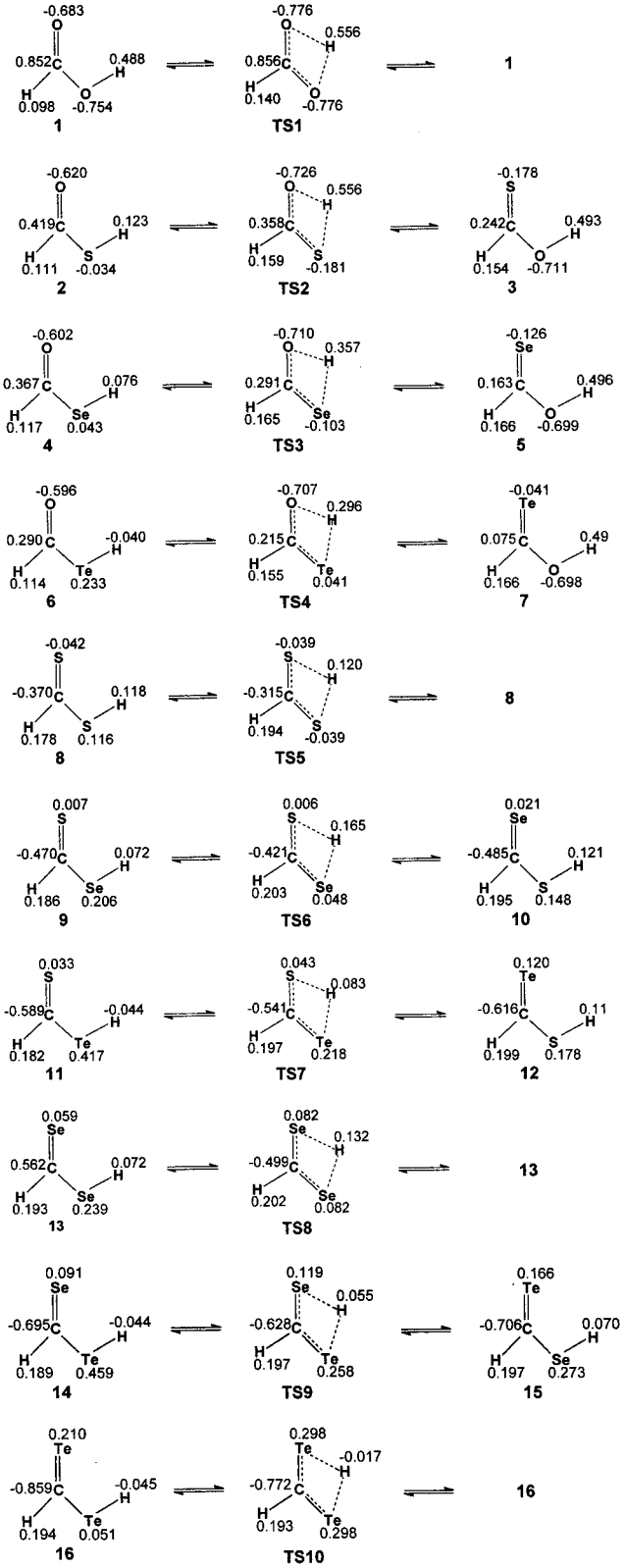

Results and Discussion

All of the acids considered in this paper are in their syn conformation because they are often the more stable ones than the corresponding anti conformers and have the right nuclear disposition for the tautomeric rearrangements. The structures **1**−**16** (Scheme 1) are minima at all levels with all eigenvalues in the Hessian matrix and the vibrational frequencies being positive except for the structure **6**, which has one imaginary

TABLE 1: Total Energies (TE) in Atomic Units, Zero-Point Vibrational Energies (ZPE) in kcal/mol, Relative Energies (RE)[a] in kcal/mol, and Dipole Moments (DPM) in Debyes of 1−16 and TS1−TS10 at the HF, MP2, and B3LYP Levels

	HF				MP2				B3LYP			
	TE	ZPE	RE	DPM	TE	ZPE	RE	DPM	TE	ZPE	RE	DPM
1	−188.819 61	23.1	0.0	1.597	−189.377 21	21.3	0.0	1.592	−189.818 33	21.2	0.0	1.425
TS1	−188.739 20	20.0	47.7	1.326	−189.320 28	18.3	32.9	1.282	−189.760 26	18.2	33.5	1.095
2	−511.449 51	18.8	0.0	1.547	−511.938 11	17.4	0.0	1.769	−512.773 49	17.4	0.0	1.346
3	−511.445 54	21.6	5.0	1.972	−511.939 71	20.1	1.6	1.725	−512.770 34	19.8	4.4	1.669
TS2	−511.374 91	17.4	45.6	1.249	−511.889 82	16.1	29.1	1.177	−512.721 28	16.0	31.4	0.927
4	−2511.648 20	17.7	0.0	1.583	−2512.159 32	16.5	0.0	1.851	−2514.059 61	16.4	0.0	1.438
5	−2511.643 67	21.1	5.9	2.217	−2512.161 96	19.6	1.1	1.841	−2514.055 24	19.4	5.7	1.691
TS3	−2511.575 09	16.6	44.9	1.377	−2512.112 39	15.5	28.5	1.262	−2514.007 69	15.3	31.5	0.982
6	−6720.937 36	16.6	0.0	1.675	−6721.423 42	15.5	0.0	1.972	−6724.240 44	15.4	0.0	1.526
7	−6720.929 87	20.7	8.3	2.619	−6721.424 05	19.2	3.1	2.081	−6724.233 53	19.0	7.9	1.757
TS4	−6720.863 10	15.9	46.0	1.452	−6721.374 52	14.8	30.0	1.299	−6724.186 56	14.7	33.1	0.994
8	−834.086 84	17.4	0.0	1.871	−834.513 11	16.3	0.0	1.960	−835.734 58	16.2	0.0	1.811
TS5	−834.024 54	15.2	37.1	0.720	−834.474 11	14.4	22.7	0.712	−835.694 96	14.1	22.8	0.526
9	−2834.285 37	16.4	0.0	1.816	−2834.734 18	15.4	0.0	1.970	−2837.019 83	15.1	0.0	1.861
10	−2834.286 22	17.0	0.0	2.087	−2834.736 96	15.9	−1.3	2.071	−2837.020 97	15.7	−0.1	1.854
TS6	−2834.226 42	14.6	35.4	0.815	−2834.698 50	13.8	20.9	0.788	−2836.983 19	13.5	21.4	0.572
11	−7043.576 18	15.3	0.0	1.851	−7043.999 99	14.4	0.0	2.050	−7047.201 32	14.2	0.0	1.961
12	−7043.575 52	16.6	1.6	2.441	−7044.004 18	15.6	−1.5	2.252	−7047.202 79	15.4	0.3	1.933
TS7	−7043.517 85	14.0	35.4	0.889	−7043.964 76	13.2	21.0	0.786	−7047.165 37	13.0	21.8	0.586
13	−4834.482 61	16.0	0.0	2.017	−4834.952 51	15.0	0.0	2.091	−4838.303 26	14.7	0.0	1.945
TS8	−4834.425 76	13.9	33.8	0.780	−4834.917 28	13.2	20.4	0.796	−4838.268 75	12.9	19.9	0.532
14	−9043.773 62	14.9	0.0	1.993	−9044.219 01	14.0	0.0	2.137	−9048.485 00	13.9	0.0	2.047
15	−9043.771 70	15.6	1.8	2.322	−9044.220 49	14.7	−0.3	2.275	−9048.484 99	14.5	0.6	2.056
TS9	−9043.717 55	13.3	33.8	0.823	−9044.185 25	12.7	20.0	0.752	−9048.451 98	12.3	19.2	0.469
16	−13 253.063 30	14.5	0.0	2.211	−13 253.488 65	13.7	0.0	2.274	−13 258.667 21	13.0	0.0	2.213
TS10	−13 253.010 00	12.8	31.9	0.636	−13 253.456 01	12.2	19.1	0.654	−13 258.637 01	11.9	17.9	0.319

[a] Scaled ZPE correction is included in RE.

frequency at the B3LYP level. The transition structures **TS1**−**TS10** have one negative eigenvalue in the Hessian matrix and one imaginary vibrational frequency each.

(1) Relative Energies. The relative energies (REs) of the optimized structures **1**−**16** and transition structures **TS1**−**TS10** calculated at the HF, MP2, and B3LYP levels of theory are given in Table 1. The zero-point vibrational energy corrections are included in the RE values.

(a) HCOXH Systems. The RE values at all levels show a thermodynamic preference for the keto moiety more than the enol moiety. This observation for thiol and thiono formic acids is in agreement with the previous experimental and theoretical assignments. Although such experimental comparisons are not available for selenium and tellurium derivatives, similar observations are expected. The values at the HF, MP2, and B3LYP levels show a preference in the order S < Se < Te. It shows that barriers decrease with decrease in electronegativity.

(b) HCSXH Systems. The equilibrium favors structures **2** over **3**. According to the results obtained at the correlated level, MP2, the structures with the C−Se (**10**) and the C═Te (**12**) double bonds are favored. At the HF level the stability follows the order **9** > **10** and **11** > **12**. But the equilibrium is almost thermoneutral at the B3LYP level. These results show relatively weak bonds between carbon and a heavier chalcogen, which would not make up a stable monomer.

(c) HCSeXH and HCTeXH Systems. The general relative stabilities between pairs with the order **4** > **5**, **9** < **10**, and **14** > **15** show a shift following the electronegativity of the chalcogens.

(d) HCX_2H Systems. The tautomeric barriers tend to decrease in order of the electronegativity of X. Thus the barrier is maximum when X = O and minimum for X = Te, with the rest falling between these two extremes.

(2) Structures of Acids. The geometrical parameters of the acids considered in this paper are given in the Table 2. Even though formic acids and thioformic acids were studied extensively, those are included here for comparison.

(a) HC(O)XH. The C−X and X−H single bond distances increase in the order O < S < Se < Te. But the C═O double-bond distance and the OCX angles are almost unaffected by various X. The CXH angles vary significantly in the order O (105.7°) > S (93.6°) > Se (92.5°) > Te (91.5°), as expected from the observed bond angles in the H_2X (X = O (104.5°), S (92°), Se (91°), Te (89.5°))[4,32,33] molecules. The OCH angles vary systematically in the order O > S > Se > Te, although the magnitude of variation is little.

(b) HC(S)XH. The single-bond distances of C−X and X−H increase in the order O < S < Se < Te. But the substitution of X has almost no effect on the C═S double-bond distance. The SCX angles show variations O (126.5°) < S (128.8°) ≈ Te (128.8°) < Se (129.0°). The variations of the CXH angles are in the order O (106.8°) > S (96.0°) > Se (94.7°) > Te (93.4°), as expected from the observed bond angles in the H_2X (X = O, S, Se, Te) molecules. As compared to HC(O)XH, the CXH angles show an increase in HC(S)XH structures. The SCH angles vary systematically in the order O > S ≈ Se > Te.

(c) HC(Se)XH. As in HC(O)XH and HC(S)XH molecules, the order O < S < Se < Te is the same for the C−X and X−H single-bond distances. But the C═Se double-bond distance and the SeCX angles are almost unaffected by various X. The CXH angles vary in the order O (107.2°) > S (96.2°) > Se (95.1°) > Te (93.9°). This observation is also as expected from the experimental bond angles in the H_2X (X = O, S, Se, Te) molecules. These are further variations compared to HC(O)XH and HC(S)XH species. The SeCH angles vary systematically in the order O > S > Se > Te, although the magnitude is little.

(d) HC(Te)XH. The variations in C−X and X−H single-bond distances are similar to other systems. The C═Te double-bond distance and the TeCX angles show insignificant changes on substituting X. The variations in the CXH angles are in the order O (107.9°) > S (96.9°) > Se (95.8°) > Te (94.6°), as expected from the observed bond angles in the H_2X (X = O,

TABLE 2: Geometries of the Structures 1−16 and the Transition Structures TS1−TS10, and the Wiberg Bond Indices at the MP2 Level. Bond Lengths are in Angstroms and Angles in Degrees. The Numbering of Atoms Follows H5−C2(=X1)−Y3−H4. Numbers in *Italics* Correspond to Experimental Values

		geometries parameters							Wiberg bond indices			
		C2−X1	C2−Y3	Y3−H4	C2−H5	X1C2Y3	C2Y3H4	X1C2H5	C2−X1	C2−Y3	Y3−H4	C2−H5
HC(O)OH	**1**[a]	1.204	1.347	0.973	1.095	125.1	105.7	125.5	1.750	1.003	0.745	0.930
		1.203	*1.342*	*0.972*	*1.097*	*124.8*	*106.3*	*123.2*				
HC(O)OH	**TS1**	1.268	1.268	1.331	1.087	112.8	71.1	123.6	1.352	1.352	0.325	0.926
HC(O)SH	**2**[b]	1.205	1.788	1.353	1.102	125.4	93.6	123.7	1.791	1.097	0.970	0.919
		1.205	*1.768*	*1.354*	*1.104*	*125.9*	*92.5*	*123.1*				
HC(S)OH	**3**	1.623	1.334	0.975	1.088	126.5	106.8	123.8	1.827	1.062	0.733	0.920
HC(O)SH	**TS2**	1.267	1.686	1.672	1.090	113.4	60.0	120.6	1.443	1.395	0.555	0.915
HC(O)SeH	**4**	1.202	1.928	1.472	1.103	125.4	92.5	123.6	1.820	1.063	0.979	0.912
HC(Se)OH	**5**	1.759	1.331	0.975	1.087	126.6	107.2	123.5	1.760	1.090	0.726	0.914
HC(O)SeH	**TS3**	1.262	1.824	1.786	1.090	113.3	57.5	120.3	1.490	1.321	0.597	0.909
HC(O)TeH	**6**	1.202	2.161	1.677	1.105	124.7	91.5	123.0	1.837	0.999	0.986	0.915
HC(Te)OH	**7**	2.009	1.287	0.975	1.087	127.4	107.9	122.8	1.619	1.113	0.723	0.924
HC(O)TeH	**TS4**	1.260	1.982	1.982	1.092	112.3	53.4	120.0	1.533	1.169	0.661	0.917
HC(S)SH	**8**[c]	1.624	1.739	1.355	1.091	128.8	96.0	121.3	1.841	1.178	0.966	0.909
		1.625	*1.733*	*1.357*	*1.100*	*127.8*	*94.3*	*121.2*				
HC(S)SH	**TS5**	1.672	1.672	1.722	1.088	115.5	67.1	122.2	1.494	1.494	0.459	0.906
HC(S)SeH	**9**	1.621	1.876	1.473	1.091	129.0	94.7	121.3	1.880	1.121	0.975	0.902
HC(Se)SH	**10**	1.760	1.731	1.357	1.090	129.1	96.2	120.6	1.761	1.215	0.960	0.904
HC(S)SeH	**TS6**	1.665	1.809	1.812	1.088	115.8	64.8	121.9	1.577	1.380	0.523	0.899
HC(S)TeH	**11**	1.622	2.097	1.679	1.092	128.8	93.4	120.7	1.916	1.022	0.982	0.909
HC(Te)SH	**12**	1.979	1.725	1.358	1.089	130.5	96.9	119.3	1.611	1.258	0.960	0.914
HC(S)TeH	**TS7**	1.662	2.030	1.984	1.089	115.7	61.1	120.5	1.671	1.190	0.601	0.909
HC(Se)SeH	**13**	1.758	1.865	1.475	1.090	129.5	95.1	120.4	1.800	1.156	0.973	0.909
HC(Se)SeH	**TS8**	1.801	1.801	1.856	1.088	116.1	66.5	121.9	1.462	1.462	0.471	0.904
HC(Se)TeH	**14**	1.761	2.082	1.680	1.090	129.3	93.9	119.7	1.837	1.052	0.982	0.916
HC(Te)SeH	**15**	1.978	1.857	1.476	1.089	130.5	95.8	119.4	1.651	1.198	0.972	0.919
HC(Se)TeH	**TS9**	1.800	2.018	2.021	1.089	116.1	62.9	120.5	1.558	1.268	0.553	0.914
HC(Te)TeH	**16**	1.981	2.072	1.680	1.090	130.5	94.6	118.6	1.692	1.088	0.981	0.926
Hc(Te)TeH	**TS10**	2.014	2.014	2.060	1.090	116.5	65.5	121.7	1.366	1.366	0.481	0.923

[a] Davis, R. W.; Robiette, A. G.; Gerry, M. C. L.; Jarnov, E. B. Winewisser, G. *J. Mol. Spectrosc.* **1980**, *81*. 93. [b] Hocking, W. H.; Winnewisser, G. *Z. Naturforsch.* **1976**, *31A*, 422, 438, 995. Hocking, W. H.; Winnewisser, G. *Z. Naturforsch.* **1977**, *32A*, 1108. [c] Bak, B.; Nielson, O. J.; Svanholt. H.; Christiansen, J. J. *J. Mol. Spectrosc.* **1979**, *75*, 134.

TABLE 3: Reaction Energies of Disproportionation Reactions (kcal/mol). Scaled ZPE Corrections Are Included

reaction	HF	MP2	B3LYP
2HC(O)SH → HC(O)OH + HC(S)SH	−2.1	−6.2	−1.2
2HC(O)SeH → HC(O)OH + HC(Se)SeH	−0.4	−3.8	1.5
2HC(O)TeH → HC(O)OH + HC(Te)TeH	−1.2	−8.2	0.4
2HC(S)SeH → HC(S)SH + HC(Se)SeH	1.3	2.2	1.8
2HC(S)TeH → HC(S)SH + HC(Te)TeH	2.7	0.0	1.3
2HC(Se)TeH → HC(Se)SeH + HC(Te)TeH	1.4	−1.3	−0.4

S, Se, Te) molecules. The TeCH angles show systematic variation in the order O > S > Se > Te, although little in magnitude.

(e) HC(X)XH. The bond parameters vary generally in the order O < S < Se < Te. Thus XCX angles follow the order O (125.1°) < S (128.8°) < Se (129.5°) < Te (130.5°). The CXH angles vary significantly in the order O (105.7°) > S (96.0°) > Se (95.1°) > Te (94.6°). The XCH angles vary systematically in the order O > S > Se > Te.

The above analysis shows that the X−H bond lengths increase on going down the chalcogenide group. This is also reflected in the occupancy and Wiberg bond indices[35] for the X−H bond (noted as the Y3−H4 bond in Table 2), which has maximum covalency on moving down the chalcogenide group. Similar covalent bonding is seen for C=X bonds. But the Wiberg bond indices of the C−X single bonds decrease only marginally on going down the group.

(3) Disproportionation Reactions. We have considered a few disproportionation reactions as given in Table 3. The monoacids HC(O)XH (X = S, Se, Te) undergo an equilibrium disproportionation reaction to form diacids. These reactions are expected to give stability to monoacids with respect to their corresponding diacids. The relative energies show that the disproportionation to the diacids is feasible when oxygen is present in the monoacid. In the absence of it, the tendency is to remain as mono acids except for HC(Se)TeH. HF and B3LYP values for relative energy are closer, while MP2 values are large. The other monoacids are not favored for disproportionation into diacids even though the RE values are closer. The relative stabilities of heavier monochalcogeno derivatives are reflected by the weak C=X and C−X bonds. Thus in general the disproportionation of monochalcogenic acids to diacids is favored provided oxygen is present. However, these conclusions are subject to further studies of intermolecular hydrogen bonding in dimers, solvent effect, etc., by experimental and theoretical methods.

(4) Natural Charge Distribution Analysis. Changes in acidity among compounds such as the above also involve changes in charge distributions. We have examined the charge distribution on tautomerization of the molecules **1**−**16** using the calculated charges based on the Weinhold−Reed natural population analysis (NPA).[36] Scheme 1 gives the natural charges on the atoms of **1**−**16** and **TS1**−**TS10**. According to this the two oxygens bear large negative charges for formic acid (**1**) in tune with the higher electronegativity of oxygen as compared to carbon and hydrogen. There is special interest in the variation of charges at the carbonyl carbon. One expects that the π-conjugative interaction would mainly increase electron density at carbon, rather than at oxygen. The observed charge distribution is $O^{-}-C^{+}-O^{-}$, leading to maximum acidity and electrostatic stabilization. The charge distribution in other species also follows the order of difference in electronegativity between interacting atoms. There is a common pattern observed with the enols **3**, **5**, and **7** as for keto derivatives **2**, **4**, and **6**. On conversion from the keto to the enol form oxygen gains

TABLE 4: Total Energies (TE) in Atomic Units, Zero-Point Vibrational Energies (ZPE) in kcal/mol, Relative Energies (RE)[a] in kcal/mol, and Dipole Moments (DPM) in Debyes of 1−8, 13, 16, and TS1−TS5 Based on Onsager's Model

	cyclohexane				THF			MeCN		
	TE	ZPE	RE	DPM	TE	RE	DPM	TE	RE	DPM
1	−188.820 09	23.1	0.0	1.702	−188.820 67	0.0	1.827	−188.820 89	0.0	1.879
TS1	−188.739 49	19.9	47.7	1.388	−188.739 82	47.9	1.460	−188.739 95	48.0	1.487
2	−511.449 88	18.8	0.0	1.667	−511.450 32	0.0	1.826	−511.450 50	0.0	1.888
3	−511.446 16	21.6	4.8	2.200	−511.446 97	4.5	2.499	−511.447 30	4.4	2.623
TS2	−511.375 11	17.4	45.7	1.323	−511.375 35	45.7	1.411	−511.375 44	45.8	1.444
4	−2511.648 50	17.7	0.0	1.697	−2511.648 87	0.0	1.841	−2511.649 01	0.0	1.896
5	−2511.644 21	21.1	5.7	2.431	−2511.644 89	5.5	2.705	−2511.645 16	5.4	2.816
TS3	−2511.575 31	16.6	44.9	1.469	−2511.575 58	45.0	1.580	−2511.575 68	45.0	1.623
6	−6720.937 61	16.6	0.0	1.793	−6720.937 92	0.0	1.935	−6720.938 04	0.0	1.990
7	−6720.930 41	20.7	8.2	2.867	−6720.931 10	7.9	3.184	−6720.931 38	7.8	3.311
TS4	−6720.863 33	15.9	46.0	1.570	−6720.863 60	46.0	1.774	−6720.863 71	46.0	1.774
8	−834.087 25	17.4	0.0	2.118	−834.087 81	0.0	2.455	−834.088 05	0.0	2.599
TS5	−834.024 60	15.2	37.4	0.759	−834.024 66	37.7	0.807	−834.024 69	37.8	0.824
13	−4834.483 05	16.0		2.325	−4834.483 67		2.777	−4834.483 94		2.973
16	−13 253.063 58	14.5		2.483	−13 253.063 94		2.483	−13 253.064 10		3.015

[a] Scaled ZPE correction is included in RE.

TABLE 5: Total Energies (TE) in Atomic Units, Zero-Point Vibrational Energies (ZPE) in kcal/mol, Relative Energies (RE)[a] in kcal/mol, and Dipole Moments (DPM) in Debyes of 1−8, 13, 16, and TS1−TS5 Based on the Self-Consistent Isodensity Polarized Continuum Model

	cyclohexane				THF			MeCN		
	TE	ZPE	RE	DPM	TE	RE	DPM	TE	RE	DPM
1	−188.823 50	23.1	0.0	1.784	−188.827 92	0.0	1.993	−188.829 57	0.0	2.073
TS1	−188.742 49	19.9	48.0	1.442	−188.746 18	48.4	1.568	−188.747 54	48.6	1.613
2	−511.452 03	18.8	0.0	1.714	−511.454 88	0.0	1.911	−511.455 93	0.0	1.985
3	−511.448 44	21.6	4.7	2.294	−511.451 97	4.3	2.708	−511.453 37	4.1	2.881
TS2	−511.376 94	17.4	45.9	1.389	−511.379 24	46.2	1.564	−511.380 10	46.3	1.633
4	−2511.650 55	17.7	0.0	1.733	−2511.653 28	0.0	1.957	−2511.654 31	0.0	2.041
5	−2511.646 86	21.1	5.3	2.641	−2511.650 84	4.6	3.216	−2511.652 47	4.2	3.470
TS3	−2511.577 10	16.6	45.1	1.550	−2511.579 43	45.4	1.769	−2511.580 31	45.5	1.858
6	−6720.939 77	16.6	0.0	1.884	−6720.942 80	0.0	2.190	−6720.943 99	0.0	2.294
7	−6720.933 45	20.7	7.6	3.195	−6720.938 06	6.6	3.989	−6720.939 97	6.2	4.319
TS4	−6720.865 12	15.9	46.2	1.644	−6720.867 49	46.6	1.893	−6720.868 40	46.8	1.997
8	−834.088 73	17.4	0.0	2.185	−834.090 95	0.0	2.571	−834.091 81	0.0	2.723
TS5	−834.025 85	15.2	37.5	0.818	−834.027 35	38.0	0.944	−834.027 92	38.1	0.996
13	−4834.484 52	16.0		2.396	−4834.486 82		2.890	−4834.487 72		3.086
16	−13 253.065 25	14.5		2.703	−13 253.067 69		3.391	−13 253.068 68		3.688

[a] Scaled ZPE correction is included in RE.

electron density to the tune of 0.1*e*. The same gain in electron density holds for C, S, Se, and Te. Thus the carbon attached to the hydroxyl (−OH) group gains electron density compared to the isomer having a keto group. The hydrogen of the −OH group becomes more positive, indicating that the enols are more acidic than the keto forms. This is expected from charge distribution and classical polarizability of atoms. The observed charge distributions clearly point to the increased acidity in the series in part by moving oxygen for other chalcogens.

(5) Solvent Effects. In general the molecules are stabilized by solvents, and the degree of stabilization depends on the size and the charge distribution in the molecule. A localized charge tends to be strongly stabilized, whereas a delocalization of charge would reduce the stabilization. The solvent effects on the reaction can be due to many reasons. The dielectric nature of the medium or the ability to form weak bonding interactions with the solute molecules may control solvent effects. The solvent dielectric media have been emulated with solvents of dielectric constants 2.0, 7.6, and 35.9. The calculations are carried out at the HF level, and the total energies, the relative energies, and the dipole moments are given in Table 4 and Table 5. A comparative analysis of these results with those of the isolated gas phase monomers shows that the dielectric medium does not affect the thermodynamic stability of the monomers and the tautomeric barriers. Thus no solvent effect could be observed due to the dielectric medium to alter the position of equilibrium as calculated using the SCRF method. It may be that weak hydrogen bond interactions between HC(X)YH and the polar molecules of the solvent (specific solvation) are controlling the thermodynamic equilibrium of these chalcogeno formic acid derivatives in solution. Table 6 shows that stabilization due to solvation is more for the enols with a lower s/p hybridization (sp^2) of oxygen than enones with a higher s/p

TABLE 6: Energies of Solvation (kcal/mol) as the Magnitude of Difference between the Total Energies of the Gas Phase and the Solvated Molecules Using SCI-PCM. Values in Parentheses Are Energies of Solvation (kcal/mol) Using Onsager's Solvation Model

	cyclohexane	THF	MeCN
1	2.44 (0.30)	5.21 (0.67)	6.50 (0.80)
TS1	2.06 (0.18)	4.38 (0.39)	5.23 (0.47)
2	1.58 (0.23)	3.37 (0.51)	4.03 (0.62)
3	1.82 (0.39)	4.03 (0.90)	4.91 (1.10)
TS2	1.27 (0.13)	2.72 (0.28)	3.26 (0.33)
4	1.47 (0.19)	3.19 (0.42)	3.83 (0.51)
5	2.00 (0.34)	4.50 (0.77)	5.52 (0.93)
TS3	1.26 (0.14)	2.72 (0.31)	3.28 (0.37)
6	1.51 (0.16)	3.41 (0.35)	4.16 (0.43)
7	2.25 (0.34)	5.14 (0.77)	6.34 (0.95)
TS4	1.27 (0.14)	2.75 (0.31)	3.33 (0.38)
8	1.19 (0.26)	2.58 (0.61)	3.12 (0.76)
TS5	0.82 (0.04)	1.76 (0.08)	2.12 (0.09)
13	1.20 (0.28)	2.64 (0.67)	3.21 (0.83)
16	1.22 (0.18)	2.75 (0.40)	3.38 (0.50)

TABLE 7: Total Energies (TE) in Atomic Units, Zero-Point Vibrational Energies (ZPE) in kcal/mol, Relative Energies (RE)[a] in kcal/mol, and Dipole Moments (DPM) in Debyes of Monochalcogenic Acetic Acids Based on the Self-Consistent Isodensity Polarized Continuum Model at the HF Level. Values in *Italics* Are at the B3LYP Level

	cyclohexane				THF			MeCN		
	TE	ZPE	RE	DPM	TE	RE	DPM	TE	RE	DPM
$CH_3C(O)SH$[b]	−550.506 624	37.4	0.0	1.994	−550.508 85	0.0	2.191	−550.509 79	0.0	2.266
	−552.109 92	*34.8*	*0.0*	*1.796*	*−552.111 98*	*0.0*	*1.977*	*−552.112 72*	*0.0*	*2.045*
$CH_3C(S)OH$	−550.502 10	40.2	5.1	2.764	−550.505 42	4.7	3.173	−550.506 74	4.4	3.328
	−552.105 72	*37.4*	*5.1*	*2.326*	*−552.108 23*	*4.9*	*2.673*	*−552.109 21*	*4.7*	*2.815*
$CH_3C(O)SeH$	−2550.705 96	36.4	0.0	2.126	−2550.708 45	0.0	2.329	−2550.709 35	0.0	2.407
	−2553.397 36	*33.9*	*0.0*	*2.010*	*−2553.399 31*	*0.0*	*2.215*	*−2553.400 03*	*0.0*	*2.295*
$CH_3C(Se)OH$	−2550.701 69	39.7	5.6	3.211	−2550.705 50	4.8	3.768	−2550.707 04	4.3	3.998
	−2553.391 82	*36.9*	*6.4*	*2.481*	*−2553.394 43*	*6.0*	*2.916*	*−2553.395 47*	*5.8*	*3.089*
$CH_3C(O)TeH$	−6759.995 83	35.3	0.0	2.318	−6759.998 40	0.0	2.590	−6759.999 37	0.0	2.686
	−6763.579 30	*33.1*	*0.0*	*2.224*	*−6763.581 29*	*0.0*	*2.492*	*−6763.582 04*	*0.0*	*2.608*
$CH_3C(Te)OH$	−6759.989 24	39.3	7.7	3.973	−6759.993 67	6.6	4.775	−6759.995 60	6.0	5.162
	−6763.570 64	*36.5*	*8.7*	*2.754*	*−6763.573 29*	*8.3*	*3.314*	*6763.574 38*	*8.1*	*3.557*

[a] Scaled ZPE correction is included in RE. [b] $CH_3C(O)SH$ is a minimum at the HF level, while it is not a minimum with an imaginary frequency of 37i for methyl rotation at the B3LYP level.

hybridization (sp) of oxygen. But this larger stabilization of enol oxygen is not sufficient to reverse the thermodynamic stability. Comparing Onsager's model and the SCI-PCM, there is a larger increase in the magnitude of the solvation energy and the dipole moment in the latter model than the former. The solvation model represented by the SCI-PCM has thus shown to be a better model than an unrealistic solvation energy calculated using Onsager's model. The dipole moments show changes depending on the dielectric constant of the solvent medium applied. While the changes of dipole moments are significant on going from gas phase to cyclohexane and in turn to THF, the changes are small from THF to MeCN. It may then be inferred that beyond a certain higher dielectric constant of the solvent the effect of solvent on dipole moment has diminished. This result is interesting in view of their potential implications on reaction mechanisms.

(6) Comparison of Solvent Effects with Monochalcogenic Acetic Acids, CH_3CXOH (X = S, Se, Te). As noted in the Introduction, experimentally a chalcogenoxo form is thermodynamically preferred over a chalcogenol form of chalcogenic carboxylic acids in polar solvents.[15] A similar preference had been reported for thioacetic acids. As monochalcogenic acetic acids represent chalcogenic carboxylic acids effectively, we have extended SCRF calculations using SCI-PCM. Calculations are performed at the HF and B3LYP levels of theory using the same basis sets as for chalcogeno formic acids. Results are given in Table 7. We have used the following conformers of monochalcogenic acetic acids for the calculation.

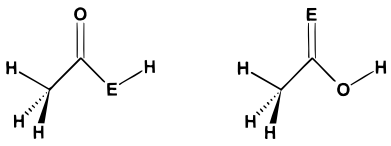

The results indicate that the chalcogenol form is still preferred both in the gas phase and in the solvent model studies. This is not in tune with the experimental results. One of the possible reasons for this is the specific solvation arising from hydrogen bonds which are indeed stronger in the hydroxy form. Further studies of hydrogen-bonded adducts of monochalcogenic acids with solvent molecules are required for a better understanding of this effect.

We have also carried out nuclear magnetic resonance (NMR) chemical shift calculations using the gauge independent atom orbital (GIAO)[37] method at the B3LYP/6-311+G(2D,P)//B3LYP/6-31G(D) level for thioacetic acids. The values are 233.8 ppm ($C_{C=S}$) and 8.5 ppm (H_{O-H}) for thiono acetic acid and 203.9 ppm ($C_{C=O}$) and 4.5 ppm (H_{S-H}) for thiol acetic acid. Relevant peaks observed experimentally were at 195.5 ppm for ^{13}C NMR and 6.4 ppm for ^{1}H NMR at all temperatures.[15] Comparison with theory assigns these peaks for thiol acetic acid. The new peaks observed experimentally at lower temperatures were at 221.2 and 14.4 ppm. This could be assigned to thiono acetic acid. Thus theoretical and experimental chemical shift values qualitatively correlate with the presence of thiono acetic acid at lower temperatures. However the intensity of ^{13}C NMR signals seen experimentally (Figure 3c of ref 15) clearly indicates that the population of thiol acetic acid is higher. This is in contrast to the results reported by Kato et al.[15]

Conclusions

A systematic analysis of HC(X)YH, (X, Y = O, S, Se, Te) molecules demonstrates periodic variations on substitution of various chalcogens. The relative energies of minima and transition structures show that the barrier for tautomerism is reduced as the electronegativity of chalcogens is decreased. The electron correlation as calculated at the MP2 and B3LYP levels has significantly reduced the barrier compared to that at the HF level. MP2 and B3LYP methods provide comparable results for relative energies and reaction barriers. The solvent effects on tautomeric equilibrium are assessed by performing self-consistent reaction field calculations at the SCF level. Onsager's solvation model has proved to be improper for the present class of molecules in solvents of lower and higher dielectric solvents. On the other hand SCI-PCM provides a better picture for the solvation and the considered molecules behave as expected from the model. However, the solvents with dielectric constants 2.0, 7.6, and 35.9 are shown to be less effective on the equilibrium of these intramolecular 1,3-H shift reactions. The dipole moments show significant variations between solvents of lower dielectric medium, while the variations are insignificant between solvents of higher dielectric media. Finally SCI-PCM calculations at the HF and B3LYP levels indicate that monochalcogenic acetic acids follow the trends of formic acid derivatives. ^{13}C and ^{1}H NMR chemical shift calculations on thioacetic acid agree with the experimental NMR spectra.

Acknowledgment. We are grateful to the University Grants Commission and the Department of Science and Technology, New Delhi, India, for the financial support. J.L. acknowledges NSF, AHPCRC, and the Mississippi Center for Supercomputing Research. E.D.J. and K.T.G. thank MHPCC for a grant of computer time. We thank a referee for helpful suggestions.

References and Notes

(1) *Organoselenium Chemistry*; Liotta, D., Ed.; John Wiley: New York, 1987.

(2) (a) Krief, A.; Hevesi, L. *Organoselenium Chemistry I*; Springer-Verlag: Berlin, 1988. (b) Irgolic, K. S. *The Organic Chemistry of Tellurium*; Gordon and Breach Science Publishers: New York, 1974.

(3) *The Chemistry of Organic Selenium and Tellurium Compounds*; Patai, S., Rappoport, Z., Eds.; John Wiley: New York, 1986.

(4) Bignall, K. W. *The Chemistry of Selenium, Tellurium, and Polonium*; Elsevier: Amsterdam, 1966.

(5) (a) Storer, A. C.; Murphy, W. F.; Carey, P. R. *J. Biol. Chem.* **1979**, *254*, 3163. (b) Lowe, G.; Williams, A. *J. Biochem.* **1965**, *96*, 189. (c) Carey, P. R.; Storer, A. C. *Pure Appl. Chem.* **1985**, *57*, 225. (d) Huber, C. P.; Ozaki, Y.; Pliura, D. H.; Storer, A. C.; Carey, P. R. *Biochemistry* **1982**, *21*, 3109.

(6) Peterson, M. R.; Csizmadia, I. G. *J. Am. Chem. Soc.* **1979**, *110*, 1076.

(7) Koller, J.; Hadzi, D.; Azman, A. *J. Mol. Struct.* **1973**, *17*, 157.

(8) Fausto, R.; Batista de Carvalho, L. A. E.; Teixeira-Dias, J. J. C.; Ramos, M. N. *J. Chem. Soc., Faraday Trans. 2* **1989**, *85*, 1945.

(9) Nguyen, M. T.; Weriga, W. D.; Ha, T. K. *J. Phys. Chem.* **1989**, *93*, 7956.

(10) (a) Yamabe, T.; Akagi, K.; Nagata, S.; Kato, H.; Fukui, K. *J. Phys. Chem.* **1976**, *80*, 611. (b) Randhawa, H. S.; Rao, C. N. R. *J. Mol. Struct.* **1974**, *21*, 123.

(11) (a) Nagata, S.; Yamabe, T.; Fukui, K. *J. Phys. Chem.* **1975**, *79*, 2335. (b) Kohlrausch, K. W. F.; Pongratz, A. *Z. Phys. Chem. B* **1934**, *27*, 176. (c) Sheppard, N. *Trans. Faraday Soc.* **1949**, *45*, 693.

(12) Teixeira-Dias, J. J. C.; Jardim-Barreto, V. M.; Ozaki, Y.; Storer, A. C.; Carey, P. R. *Can. J. Chem.* **1982**, *60*, 174.

(13) (a) Hinze, J.; Jaffé, H. H. *J. Am. Chem. Soc.* **1962**, *84*, 540. (b) Hinze, J.; Jaffé, H. H. *J. Phys. Chem.* **1963**, *67*, 1501.

(14) Pauling, L. *The Nature of the Chemical Bond*; Cornell University Press: Ithaca, 1960; pp 224−228.

(15) Kato, S.; Kawahara, Y.; Kageyama, H.; Yamada, R.; Niyomura, O.; Murai, T.; Kanda, T. *J. Am. Chem. Soc.* **1996**, *118*, 1262.

(16) Fausto, R.; Batista de Carvalho, L. A. E.; Teixeria-Dias, J. J. C. *J. Mol. Struct. (THEOCHEM)* **1990**, *207*, 67.

(17) Frisch, M. J.; Trucks, G. W.; Schlegel, H. B.; Gill, P. M. W.; Johnson, B. G.; Wong, M. W.; Foresman, J. B.; Robb, M. A.; Head-Gordon, M.; Replogle, E. S.; Gomperts, R.; Andres, J. L.; Raghavachari, K.; Binkley, J. S.; Gonzalez, C.; Martin, R. L.; Fox, D. J.; Defrees, D. J.; Baker, J.; Stewart, J. J. P.; Pople, J. A. *Gaussian 92/DFT, Revision G.3*; Gaussian, Inc.: Pittsburgh, PA, 1993.

(18) Frisch, M. J.; Trucks, G. W.; Schlegel, H. B.; Gill, P. M. W.; Johnson, B. G.; Robb, M. A.; Cheeseman, J. R.; Keith, T.; Petersson, G. A.; Montgomery, J. A.; Raghavachari, K.; Al-Laham, M. A.; Zakrzewski, V. G.; Ortiz, J. V.; Foresman, J. B.; Cioslowski, J.; Stefanov, B. B.; Nanayakkara, A.; Challacombe, M.; Peng, C. Y.; Ayala, P. Y.; Chen, W.; Wong, M. W.; Andres, J. L.; Replogle, E. S.; Gomperts, R.; Martin, R. L.; Fox, D. J.; Binkley, J. S.; Defrees, D. J.; Baker, J.; Stewart, J. P.; Head-Gordon, M.; Gonzalez, C.; Pople, J. A. *Gaussian 94, Revision D.1*; Gaussian, Inc.: Pittsburgh, PA, 1995.

(19) Møller, C.; Plesset, M. S. *Phys. Rev.* **1934**, *46*, 618.

(20) Stephens, P. J.; Delvin, F. J.; Chabalowski, C. F.; Frisch, M. J. *J. Phys. Chem.* **1994**, *98*, 11623.

(21) Becke, A. D. *J. Chem. Phys.* **1993**, *98*, 5648.

(22) Lee, C.; Yang, W.; Parr, R. G. *Phys. Rev. B* **1988**, *37*, 785.

(23) Vosoko, S. H.; Wilk, L.; Nusair, M. *Can. J. Phys.* **1980**, *58*, 1200.

(24) Hehre, W. J.; Radom, L.; Schleyer, P. v. R.; Pople, J. A. *Ab Initio Molecular Orbital Theory*; Wiley Interscience: New York, 1986.

(25) Huzinga, S.; Andzelm, J.; Klobukowski, M.; Radzio-Andzelm, E.; Sakai, Y.; Tatewaki, H. *Gaussian Basis Sets for Molecular Calculations*; Elsevier: Amsterdam, 1984.

(26) Urban, J.; Schreiner, P. R.; Vacek, G.; Scleyer, P. v. R.; Huang, J. Q.; Leszczynski, J. *Chem. Phys. Lett.* **1997**, *264*, 441.

(27) Wong, M. W.; Frisch, M. J.; Wiberg, K. B. *J. Am. Chem. Soc.* **1991**, *113*, 4776.

(28) Wong, M. W.; Wiberg, K. B.; Frisch, M. J. *J. Am. Chem. Soc.* **1992**, *114*, 523.

(29) Wong, M. W.; Wiberg, K. B.; Frisch, M. J. *J. Am. Chem. Soc.* **1992**, *114*, 1645.

(30) Foresman, J. B.; Frisch, A. *Exploring Chemistry with Electronic Structure Methods*; Gaussian, Inc.: Pittsburgh, PA, 1996.

(31) (a) Miertus, S.; Scocco, E.; Tomasi, J. *J. Chem. Phys.* **1981**, *55*, 117. (b) Tomasi, J.; Bonaccorsi, R.; Cammi, R.; Valle, F. O. *J. Mol. Struct.* **1991**, *234*, 401. (c) Tomasi, J.; Persico, M. *Chem. Rev.* **1994**, *94*, 2027.

(32) Murov, L. S. *Handbook of Photochemistry*; Marcel Dekker, Inc.: New York, 1973.

(33) Edwards, T. H.; Moncur, N. K.; Snyder, L. E. *J. Chem. Phys.* **1967**, *46*, 2139.

(34) Bailar, J. C., Jr.; Emeleus, H. J.; Nyholm, R.; Trotman-Dickenson, A. F. *Comprehensive Inorganic Chemistry*; Pergamon Press: New York, 1973; Vol. 2.

(35) (a) Wiberg, K. B. *Tetrahedron* **1968**, *24*, 1083. (b) Mayer, I. *Theor. Chim. Acta* **1985**, *67*, 315.

(36) (a) Reed, A. E.; Weinstock, R. B.; Weinhold, F. A. *J. Chem. Phys.* **1985**, *83*, 735. (b) Reed, A. E.; Weinhold, F. A.; Curtiss, L. A. *Chem. Rev.* **1988**, *88*, 899.

(37) (a) Wolinski, K.; Hilton, J. F.; Pulay, P. *J. Am. Chem. Soc.* **1990**, *112*, 8251. (b) Dodds, J. L.; McWeeny, R.; Sadlej, A. J. *Mol. Phys.* **1980**, *41*, 1419. (c) Ditchfield, R. *Mol. Phys.* **1974**, *27*, 789. (d) McWeeny, R. *Phys. Rev.* **1962**, *126*, 1028. (e) London, F. *J. Phys. Radium, Paris* **1937**, *8*, 397.